Chapter 1

Introduction

The history of wind wave research is relatively short. Although there were basic developments last century (Airy, 1845; Stokes, 1847), a concerted effort really only began as a result of the military imperative of the Second World War. The work of Sverdrup, Munk and Bretschneider (Sverdrup and Munk, 1944a,b; Bretschneider, 1952a) provided the first observational data base, upon which, to base theories for the evolution of wind generated waves. This work was, however, largely empirical. A theoretical framework began to develop with the studies of wind-wave generation by Miles and Phillips (Miles, 1957; Phillips, 1957). A more complete understanding of the full evolution process, however, awaited the insight into nonlinear interactions provided by Hasselmann (Hasselmann, 1962).

By the mid 60s, the basic processes responsible for the evolution of the wind wave spectrum had been identified. An ability to accurately predict the evolution of the spectrum awaited an increase in the observational data base and advances in computational speed.

The goals of wind wave research are relatively well defined: to be able to predict the wind wave field and its effect on the environment. That environment could be natural (beaches, the atmosphere etc.) or imposed by human endeavour (ports, harbours, coastal settlements etc.). Although the goals are similar, the specific requirements of these various fields differ. For instance, coastal engineering activity may only require knowledge of the integral parameters of significant wave height and peak period, whereas studies of air-sea interaction will generally require a very detailed description of the full spectrum.

This book attempts to summarise the current state of this knowledge and to place this understanding into a common frame work. There are still many aspects of wind waves which are not fully understood. A notable example being wave breaking. Despite this, an impressive ability now exists to predict waves on both global and regional scales. Indeed, it is the author's belief that the most significant source of error in deep water wave models is the driving wind. Further advances

in our understanding of the physics of wave evolution will result in only marginal improvements in the prediction capability. In finite depth regions, knowledge is still relatively poor and further work is clearly required.

The past 20 years has also brought enormous advances in our abilities to measure the ocean wave field. In particular, satellite based remote sensing instruments can now provide a global, real time view of the wave field. The analysis of this growing observational data base is beginning to yield the first global wave climatologies needed for activities such as shipping and ocean engineering. In addition, the assimilation of these data into wave prediction models will begin to address the deficiencies of the forcing wind fields.

This book attempts to take a balanced approach between the pragmatic engineering view of requiring a short term result and the scientific quest for detailed understanding. Thus, it attempts to provide a rigorous description of the physical processes involved as well as practical predictive tools.

A basic assumption which is made throughout the text is that, to first order, waves can be assumed linear. Nonlinearities can be considered as perturbations to this linear solution. It follows from this assumption that waves can be considered in a spectral sense. As a result, fundamentally nonlinear descriptions have been largely ignored. This approach stems from the pragmatic view that the spectral representation of waves is the only approach which has developed a comprehensive predictive capability, even in shallow water where nonlinearities increase.

Chapter 2

Wave Theory

2.1 Introduction

As a pre-curser to the investigation of the properties of waves under the active forcing of the wind, it is essential to consider the more idealized case of the wave field propagating in the absence of any forcing. Even this highly idealized situation presents formidable mathematical difficulties and thus requires many simplifying assumptions to form a tractable solution. As the restrictions of these simplifying assumptions are gradually reduced the complexity of the solution increases. Only the simplest of these solutions will be considered here. Interest will focus on linear or Airy wave theory (Airy, 1845). Despite the apparently restrictive simplifying assumptions associated with this theory, its range of application is extensive. Linear wave theory will form the basic theoretical rationale for the remainder of this book.

2.2 Small Amplitude or Linear Theory

2.2.1 Governing Equations

In order to form a tractable solution the following simplifying assumptions are made:

1. The water is of constant depth, d and wave length, L (or period, T).
2. The wave motion is two-dimensional, which leads to long crested waves with constant height along the crests.
3. The waves are of constant form, that is, they do not change with time.
4. The fluid (water) is incompressible.

5. Effects of viscosity, turbulence, and surface tension are neglected.

6. The wave height, H is small compared to the wave length, L and the water depth, d (i.e. $H/L << 1$ and $H/d << 1$).

The limitations which these assumptions place on the resulting theory will be investigated in Section (2.4).

The governing equations to be solved represent the equations for conservation of mass and momentum. Conservation of mass can be written in terms of the Laplace Equation

$$\frac{\partial^2\phi}{\partial x^2} + \frac{\partial^2\phi}{\partial z^2} = 0 \tag{2.1}$$

where x and z are the horizontal and vertical coordinates, respectively, of the two-dimensional solution domain. The velocity potential, ϕ is defined in terms of the horizontal and vertical components of velocity, u and w as

$$u(x,z,t) = -\frac{\partial\phi}{\partial x} \tag{2.2}$$

$$w(x,z,t) = -\frac{\partial\phi}{\partial z} \tag{2.3}$$

and t is time.

The conservation of momentum is represented by the Unsteady Bernoulli Equation

$$-\frac{\partial\phi}{\partial t} + \frac{p}{\rho_w} + gz = 0 \tag{2.4}$$

where p is the pressure, ρ_w the density of the fluid (water) and g is gravitational acceleration. It is desired to solve (2.1) and (2.4) within the domain represented by Figure 2.1 and subject to the boundary conditions defined below.

(i) Dynamic Boundary Condition at the free surface:

At the free surface, $z = \eta$, the pressure is atmospheric, $p = 0$. Therefore (2.4) becomes

$$-\frac{\partial\phi}{\partial t} + g\eta = 0 \text{ at } z = 0 \tag{2.5}$$

The boundary condition, (2.5) has been applied at $z = 0$ rather than $z = \eta$ since one of the simplifying assumptions was that the waves were of small amplitude (i.e. $\eta \rightarrow 0$).

(ii) Kinematic Boundary Condition at the free surface:

At the free surface there can be no transport of fluid through the free surface. Hence, the vertical velocity of the free surface must equal the vertical velocity of the fluid (i.e. $w = D/Dt[\eta(x,t)]$).

$$w = \underbrace{\frac{\partial\eta}{\partial t} + u\frac{\partial\eta}{\partial x}}_{\substack{\text{vertical velocity} \\ \text{of free surface}}} \quad \text{at } z = \eta \tag{2.6}$$

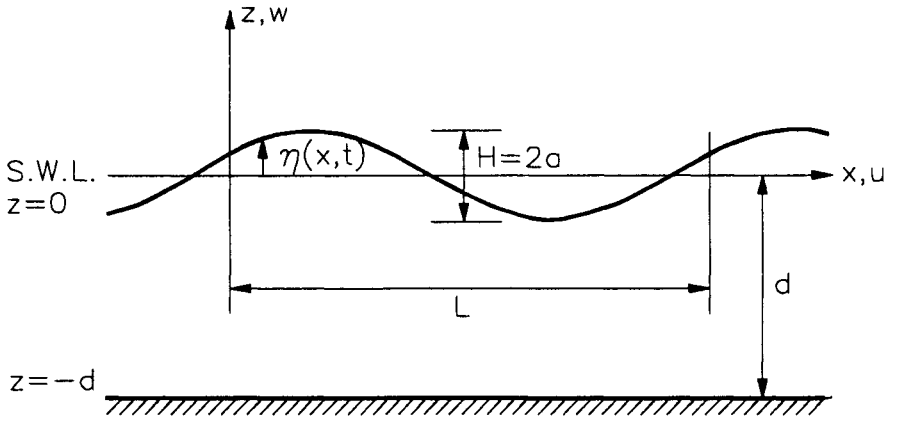

Figure 2.1: Definition sketch showing the solution domain for Linear Wave Theory

Substituting (2.3) for w, noting that due to the small amplitude assumption the slope of the water surface $\partial\eta/\partial x$ will be small and that the boundary condition can be assumed to apply at $z = 0$ reduces (2.6) to

$$-\frac{\partial\phi}{\partial z} = \frac{\partial\eta}{\partial t} \text{ at } z = 0 \tag{2.7}$$

(iii) Kinematic Boundary Condition at the bed:

In a similar fashion to the kinematic boundary condition at the free surface, there can be no flow through the solid bed

$$w = -\frac{\partial\phi}{\partial z} = 0 \text{ at z=–d} \tag{2.8}$$

Hence, the problem becomes the solution of (2.1) subject to the boundary conditions (2.5), (2.7) and (2.8). This system of equations, together with the solution domain is shown diagrammatically in Figure 2.2.

A solution to this set of equations can be found using the method of separation of variables (Airy, 1845; Stokes, 1847)

$$\phi(x,z,t) = \frac{ag}{\omega}\frac{\cosh\left[k\left(d+z\right)\right]}{\cosh\left[kd\right]}\cos\left(kx-\omega t\right) \tag{2.9}$$

where $a = H/2$ is the wave amplitude, $\omega = 2\pi/T = 2\pi f$ is the wave angular frequency and $k = 2\pi/L$ is the wave number. From (2.9) the basic properties of linear water waves can be developed. A number of these key properties are defined in Sections (2.2.2) to (2.2.9).

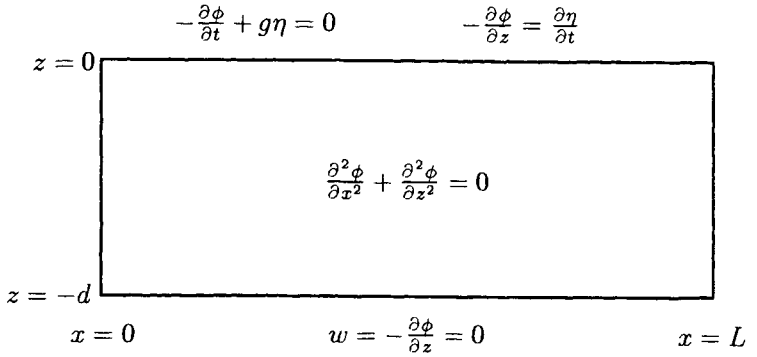

Figure 2.2: The governing equation, together with boundary conditions and the solution domain for Linear Wave Theory

2.2.2 The Wave Profile

Equation (2.5) states that at the free surface

$$\eta = \frac{1}{g}\left[\frac{\partial\phi}{\partial t}\right]_{z=0} \tag{2.10}$$

Substituting (2.9) for ϕ in (2.10) and differentiating with respect to t yields

$$\eta = a\sin(kx - \omega t) \tag{2.11}$$

Hence the water surface varies in a sinusoidal manner and is periodic in both space (wave length L) and time (period T).

2.2.3 Dispersion Relationship

Combining (2.5) and (2.7) yields

$$-\frac{\partial\phi}{\partial z} = \frac{1}{g}\frac{\partial^2\phi}{\partial t^2} \text{ at } z = 0 \tag{2.12}$$

Substituting (2.9) in (2.12) and evaluating at $z = 0$ yields

$$\omega^2 = gk\tanh(kd) \tag{2.13}$$

Equation (2.13) is called the "dispersion relationship" for linear waves. It states that there is a unique relationship between ω, k and d (or T, L and d). If two of the quantities are know, the third is uniquely defined.

2.2.4 Wave Phase Speed

By definition, the phase speed or speed of propagation, C of a wave is

$$C = \frac{L}{T} \text{ or } \frac{\omega}{k} \tag{2.14}$$

Substituting (2.13) in (2.14) for ω yields

$$C^2 = \frac{g}{k} \tanh(kd) \tag{2.15}$$

The phase speed, as defined by (2.15) is sometimes also called the "celerity". Equation (2.15) indicates that the phase speed varies with water depth. For given values of ω and k the wave will propagate faster in deep water than in shallow water. Also, C varies as a function of ω or k. Long period or long wave length waves will propagate faster than short period or short wave length waves. Hence, if a group of waves of varying wave length were to propagate away from an area where they were initially generated, they would propagate at different speeds. The longer wave length waves would propagate faster than the shorter wave length waves. The waves would gradually separate based on there respective wave lengths. The longer waves would lead followed by progressively shorter waves. Hence, the wave field would gradually disperse. This gives rise to the name, "dispersion relationship" attributed to (2.13).

2.2.5 Wave Length

Similarly, substituting (2.14) into (2.15) yields a transcendental relationship for the wave length, L

$$L = \frac{gT^2}{2\pi} \tanh\left(\frac{2\pi d}{L}\right) \tag{2.16}$$

The transcendental nature of (2.13), (2.15) and (2.16) means that iterative solution techniques are required. For this reason, a range of approximations have been proposed for the determination of C or k given ω and d. Hunt (1979) proposed a Padé approximation of the form

$$\frac{C^2}{gd} = \left[\tilde{\omega} + \left(1 + 0.666\tilde{\omega} + 0.445\tilde{\omega}^2 - 0.105\tilde{\omega}^3 + 0.272\tilde{\omega}^4\right)^{-1}\right]^{-1} \tag{2.17}$$

where $\tilde{\omega} = \omega^2 d/g$. Equation (2.17) is a remarkably accurate approximation to (2.16). Indeed, it is derived so as to be exact at both the short and long wave length limits. Young and Sobey (1980) have also suggested the use of a table look-up scheme for the routine evaluation of C within computer codes. Fenton and McKee (1990) have presented an extensive review of a number of different approximations which have been proposed. They conclude that there is little practical difference been the accuracy of the various approximations.

2.2.6 Water Particle Motion

The horizontal and vertical components of the fluid velocity (water particle velocity) are defined by (2.2) and (2.3). Substitution of (2.9) into these relationships yields

$$u = \frac{agk}{\omega} \frac{\cosh\left[k\left(d+z\right)\right]}{\cosh\left(kd\right)} \sin\left(kx - \omega t\right) \tag{2.18}$$

$$w = -\frac{agk}{\omega} \frac{\sinh\left[k\left(d+z\right)\right]}{\cosh\left(kd\right)} \cos\left(kx - \omega t\right) \tag{2.19}$$

The horizontal and vertical displacement of a fluid particle can be defined as

$$\xi = \int u dt \; ; \; \zeta = \int w dt \tag{2.20}$$

Substitution of (2.18) and (2.19) into (2.20) and integrating yields

$$\xi = \frac{agk}{\omega^2} \frac{\cosh\left[k\left(d+z\right)\right]}{\cosh\left(kd\right)} \cos\left(kx - \omega t\right) \tag{2.21}$$

$$\zeta = \frac{agk}{\omega^2} \frac{\sinh\left[k\left(d+z\right)\right]}{\cosh\left(kd\right)} \sin\left(kx - \omega t\right) \tag{2.22}$$

In (2.21) and (2.22) ξ and ζ are measured from the mean position.

Substituting the dispersion relationship (2.13) for ω^2 in (2.21) and (2.22), these relationships can be re-arranged to yield

$$\frac{\xi^2}{A^2} + \frac{\zeta^2}{B^2} = 1 \tag{2.23}$$

where

$$A = a \frac{\cosh\left[k\left(d+z\right)\right]}{\sinh\left(kd\right)} \tag{2.24}$$

$$B = a \frac{\sinh\left[k\left(d+z\right)\right]}{\sinh\left(kd\right)} \tag{2.25}$$

Equation (2.23) represents an ellipse with horizontal semi-axis A and vertical semi-axis B. Therefore, for linear wave theory, fluid particles move in closed elliptical orbits. In deep water $A = B$ and the orbit becomes a circle. This motion is shown diagrammatically in Figure 2.3.

Figure 2.4 shows the ratio of the horizontal to vertical components of velocity and displacement, u/w and ξ/ζ, respectively as a function of the parameter $k(d+z)$. As shown in Figure 2.3, the orbits progressively become more elongated with decreasing depth, d and submergence z. Indeed, at the bottom, $z = -d$, the kinematic boundary condition (2.8) requires that $w = 0$ and hence both u/w and $\xi/\zeta \rightarrow \infty$ for small $k(d+z)$.

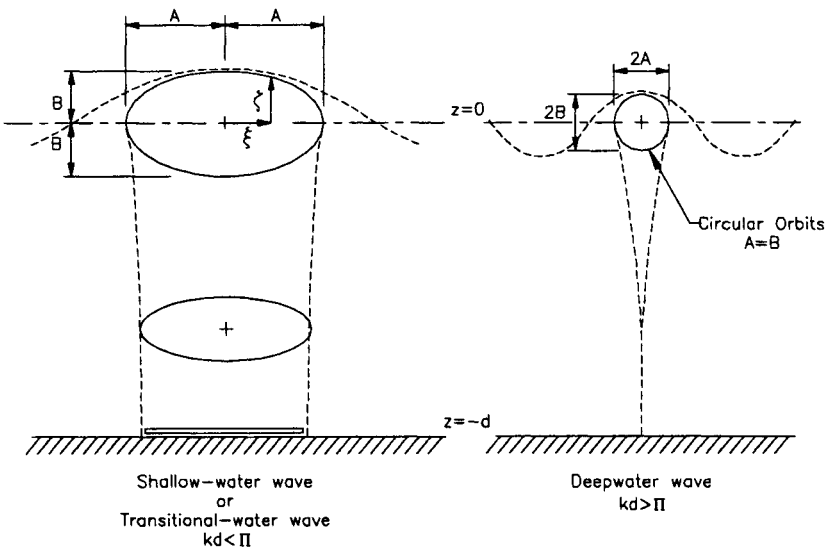

Figure 2.3: Diagrammatic representation of the motion of a fluid particle beneath a wave as predicted by linear wave theory [after CERC (1984)].

2.2.7 Pressure

Substitution of the velocity potential, ϕ from (2.9) into the Unsteady Bernoulli Equation (2.4) and differentiating yields

$$\frac{p}{\rho_w} = \frac{g\cosh\left[k\left(d+z\right)\right]}{\cosh\left(kd\right)} \underbrace{a\sin\left(kx-\omega t\right)}_{=\eta} - gz \tag{2.26}$$

Noting that from, (2.11), $\eta = a\sin(kx-\omega t)$, (2.26) becomes

$$\frac{p}{\rho_w g} = \underbrace{\eta \frac{\cosh\left[k\left(d+z\right)\right]}{\cosh\left(kd\right)}}_{=K_p} - z \tag{2.27}$$

or

$$\frac{p}{\rho_w g} = K_p\eta - z \tag{2.28}$$

where K_p is called the pressure response factor. The first term in (2.28) represents either a positive or negative (depending on the phase of the wave) deviation from hydrostatic pressure. In addition, the value of K_p decreases with increasing $|z|$ and hence the pressure fluctuations associated with the presence of the surface waves decrease with increasing distance below the water surface. For deep water conditions ($d \rightarrow \infty$), the value of K_p reduces from 1 at $z = 0$ to 0.04 at $z = -L/2$.

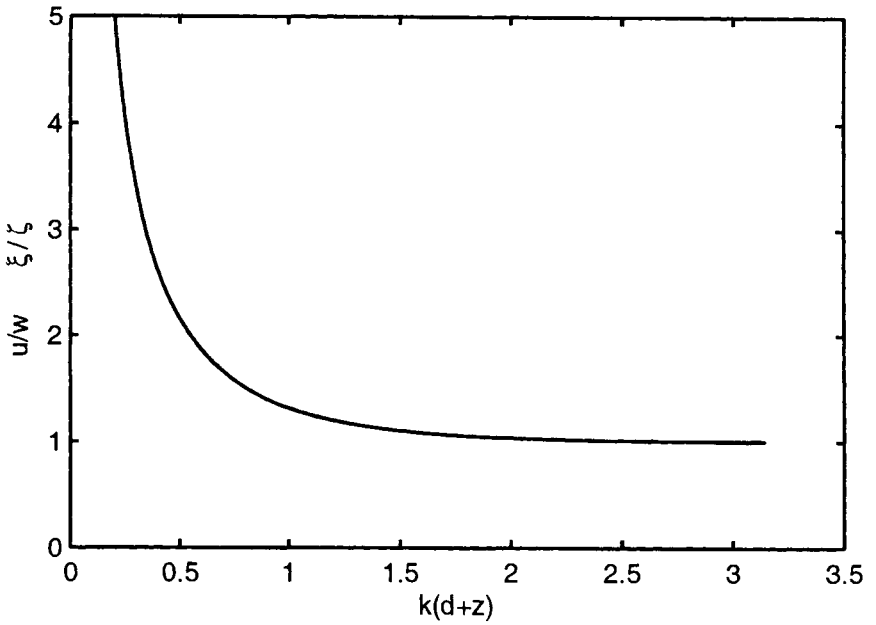

Figure 2.4: Ratio of the horizontal to vertical components of velocity, (u/w) and displacement (ξ/ζ) as a function of $k(d+z)$.

Hence, the influence of the surface waves is negligible at depths of submergence greater than approximately $L/2$.

2.2.8 Classification with respect to Depth

The hyperbolic functions which appear in the relationships of linear wave theory provide a convenient mechanism for the classification of waves with respect to water depth. The values of these hyperbolic functions as the argument kd approaches zero and infinity, respectively are shown in Table 2.1.

The asymptotic limits shown in Table 2.1 enable the linear wave relationships to be simplified for the limits of small and large values of kd. Arbitrary limits have been set for the values of kd (or $2\pi d/L$) at which the asymptotic relationships can be used with reasonable accuracy. These values are shown in Table 2.2. Use of the asymptotic relationships result in errors not exceeding 5% for the hyperbolic functions at the limits shown. The practice of classification of waves with respect to water depth is largely historical. Before the advent of modern computers, the evaluation of the hyperbolic functions and the transcendental relationships associated with linear wave theory was a tedious process. For the limits of deep and shallow water, these relationships could be significantly simplified. The classification system, and the resulting simplifications still find application today. Many mathe-

Function	Value of function as $kd \to 0$	Value of function as $kd \to \infty$
$\sinh kd$	kd	$e^{kd}/2$
$\cosh kd$	1	$e^{kd}/2$
$\tanh kd$	kd	1

Table 2.1: Asymptotic limits of the linear wave theory hyperbolic functions.

Range of kd	Range of d/L	Type of waves
0 to $\pi/10$	0 to 1/20	Shallow water waves (long waves)
$\pi/10$ to π	1/20 to 1/2	Intermediate depth waves
π to ∞	1/2 to ∞	Deep water waves (short waves)

Table 2.2: Depth classification of linear waves in terms of the relative depth parameter kd.

matical manipulations involving linear wave relationships yield analytical solutions with the assumption of either deep or shallow water wave conditions. In addition, the classification system provides a physical interpretation of when bottom effects may influence wave properties. An example of this might be to what extent data collected in deep water might be applicable in finite depth situations. Table 2.2 also indicates that the depth, d is not the sole parameter which determines whether waves are in deep or shallow water. It is the relative depth parameter, kd, which provides this measure. The wave number, k (or wave length L) determines the depth to which the orbital velocities, accelerations and pressure are significant. Hence, it is the product kd which defines whether interaction with the bottom will influence the wave properties. A full summary of the linear wave relationships and their deep and shallow water simplifications is shown in Table 2.3.

RELATIVE DEPTH	**SHALLOW WATER** $kd < \pi/10$	**TRANSITIONAL WATER** $\pi/10 < kd < \pi$	**DEEP WATER** $kd > \pi$
Wave profile	Same as $\longrightarrow$	$\eta = a\sin(kx - \omega t)$	Same as $\longleftarrow$
Phase speed	$C = \sqrt{gd}$	$C = \frac{g}{\omega}\tanh(kd)$	$C = \frac{g}{\omega}$
Wave length	$L = T\sqrt{gd}$	$L = \frac{gT^2}{2\pi}\tanh\left(\frac{2\pi d}{L}\right)$	$L = \frac{gT^2}{2\pi}$
Angular frequency	$\omega^2 = gk^2 d$	$\omega^2 = gk\tanh(kd)$	$\omega^2 = gk$
Group velocity	$C_g = \sqrt{gd}$	$C_g = \frac{1}{2}\left[1 + \frac{2kd}{\sinh(2kd)}\right]C$	$C_g = \frac{g}{2\omega}$
Velocity components	$u = a\sqrt{\frac{g}{d}}\sin\psi$	$u = \frac{agk}{\omega}\frac{\cosh[k(d+z)]}{\cosh(kd)}\sin\psi$	$u = a\omega e^{kz}\sin\psi$
	$w = a\omega\left(1 + \frac{z}{d}\right)\cos\psi$	$w = -\frac{agk}{\omega}\frac{\sinh[k(d+z)]}{\cosh(kd)}\cos\psi$	$w = -a\omega e^{kz}\cos\psi$
Particle displacements	$\xi = \frac{a}{\omega}\sqrt{\frac{g}{d}}\cos\psi$	$\xi = \frac{agk}{\omega^2}\frac{\cosh[k(d+z)]}{\cosh(kd)}\cos\psi$	$\xi = ae^{kz}\cos\psi$
	$\zeta = a\left(1 + \frac{z}{d}\right)\sin\psi$	$\zeta = -\frac{agk}{\omega^2}\frac{\sinh[k(d+z)]}{\cosh(kd)}\sin\psi$	$\zeta = -ae^{kz}\sin\psi$
Subsurface pressure	$\frac{p}{\rho_w g} = \eta - z$	$\frac{p}{\rho_w g} = \eta\frac{\cosh[k(d+z)]}{\cosh(kd)} - z$	$\frac{p}{\rho_w g} = \eta e^{kz} - z$

Table 2.3: Depth classification of linear waves in terms of the relative depth parameter kd. Note that in the above, $\psi = (kx - \omega t)$.

2.2.9 Wave Trains and Group Velocity

Equation (2.11) defines the water surface elevation of a single linear wave train. Consider now a water surface consisting of two wave trains defined by the general form (2.11). Each train has the same amplitude, a but different frequencies ω_1 and ω_2, respectively. The water surface elevation becomes

$$\eta = a\sin(k_1x - \omega_1 t) + a\sin(k_2x - \omega_2 t) \tag{2.29}$$

$$= \overbrace{2a\cos[1/2(k_1 - k_2)x - 1/2(\omega_1 - \omega_2)t]}^{\text{variable amplitude of wave train}} \times \sin[1/2(k_1 + k_2)x - 1/2(\omega_1 + \omega_2)t] \tag{2.30}$$

The first term in (2.30) represents a time and space varying amplitude of the wave train. The resulting wave train is characterized by interference patterns and the appearance of groups of waves as shown in Figure 2.5.

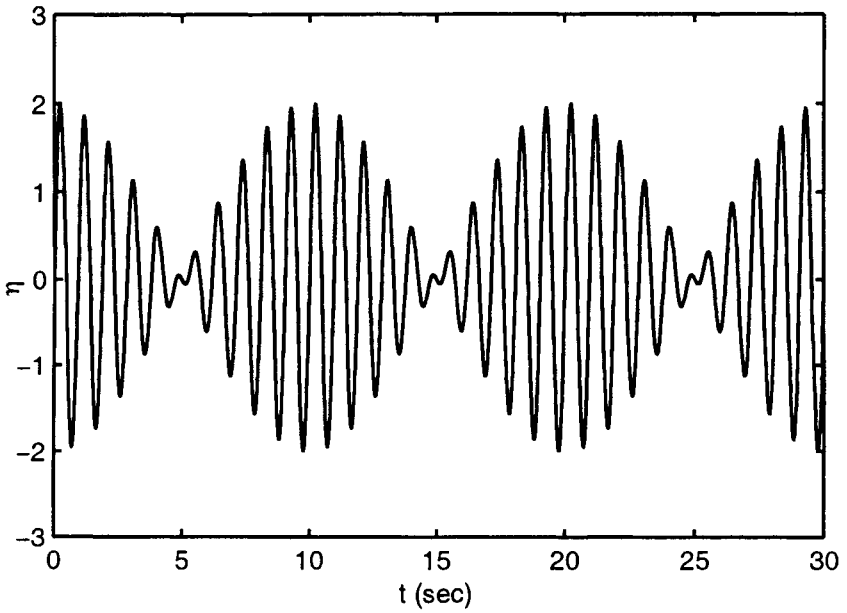

Figure 2.5: The formation of wave groups as a result of the superposition of two linear wave trains with different frequencies (Kinsman, 1965).

The water surface elevation, η is zero when the first term in (2.30) is zero. This occurs when

$$1/2(k_1 - k_2)x - 1/2(\omega_1 - \omega_2)t = (2m + 1)\pi/2 \tag{2.31}$$

where m is an integer counter (i.e. $m = 0, 1, 2, \cdots$). Therefore, the envelope

(Figure 2.5) to the water surface elevation will be zero at $x = x_{node}$ given by

$$x_{node} = \left[\frac{\omega_1 - \omega_2}{k_1 - k_2}\right] t + \frac{(2m+1)\,\pi}{k_1 - k_2} \tag{2.32}$$

The speed of propagation of the nodal point and hence the wave "group" is

$$C_g = \frac{\mathrm{d}x_{node}}{\mathrm{d}t} = \frac{\omega_1 - \omega_2}{k_1 - k_2} \tag{2.33}$$

where C_g is called the group velocity. In the limit as ω_1 approaches ω_2, (2.33) becomes

$$C_g = \frac{\mathrm{d}\omega}{\mathrm{d}k} \tag{2.34}$$

Substituting the dispersion relationship (2.13) into (2.34) and differentiating yields

$$C_g = \underbrace{\frac{1}{2}\left[1 + \frac{2kd}{\sinh(2kd)}\right]}_{n} C \tag{2.35}$$

where

$n \longrightarrow 1/2$ in deep water
$n \longrightarrow 1$ in shallow water

Hence, the group velocity is half the phase speed in deep water and equal to the phase speed in shallow water. The variation in the ratio C_g/C is shown in Figure 2.6 as a function of the relative depth parameter kd.

In all but shallow water, the individual waves in the group are propagating faster than the group itself. The individual waves will appear at the rear of the group, propagate through the group and disappear at the front of the group. If a single group of waves propagating on an otherwise calm ocean is considered, individual waves will be observed to propagate through the group at their phase speed, C. The group will, however, remain intact and continue to propagate at the group velocity, C_g. Hence, the energy represented by the group will propagate at the speed of translation of the group rather than the individual waves that make up the group (Svendsen and Jonsson, 1976). Wave energy propagating from a generation site travels at the group velocity rather than the phase speed.

2.3 Wave Transformation

2.3.1 Basic Assumptions

Previously, only cases where the water depth was constant were considered. Indeed, the specification of the governing equation together with the appropriate boundary conditions [(2.1), (2.5), (2.7) and (2.8)] requires that d = constant. To a reasonable

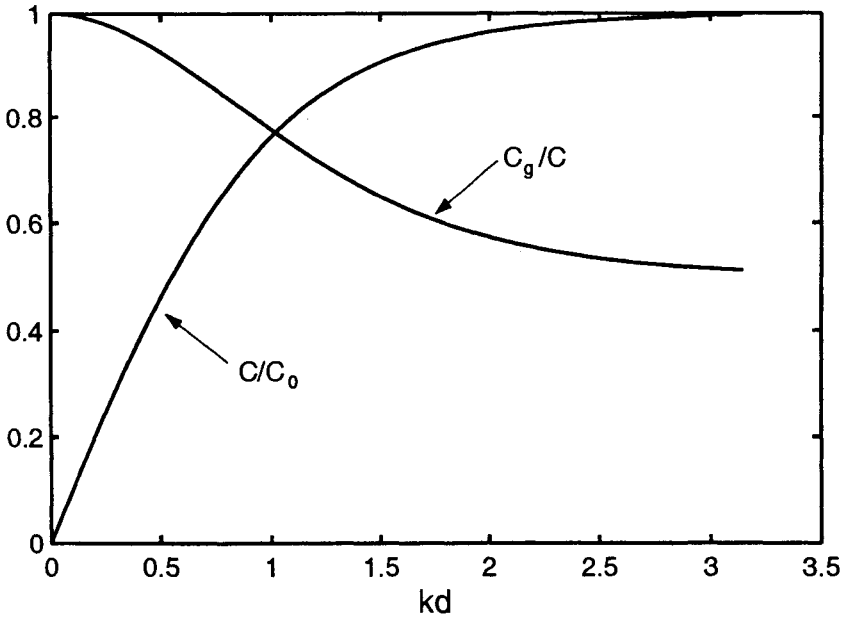

Figure 2.6: Variation in the ratio of group velocity to phase speed (C_g/C) and phase speed to deep water phase speed (C/C_0) as functions of the relative depth parameter kd.

level of accuracy, this condition may be relaxed provided that the depth varies only slowly on a scale given by the wave length. There is no absolute limit to how rapidly the bottom can vary whilst linear wave theory remains a reasonable approximation. The problem has been investigated by numerous authors including Rosseau (1952),Ogawa and Yashida (1959), Madsen and Mei (1969a,b). It appears that linear theory remains a reasonable approximation provided that the water depth changes by less than 20% to 30% within one wave length (Svendsen and Jonsson, 1976).

Consider the case of waves propagating towards the shore from deep to shallow water. Two points of different water depth can be specified along this propagation path and the number of waves passing each point can be counted over some finite period of time. As the individual waves must be conserved, the number of waves passing each point must be the same. The wave period, T, as defined in Section (2.2.2) is the time taken for successive waves to pass a fixed point. As the number of waves passing the two selected points is the same during the finite time period, the wave period at the two points must also be the same. Hence, as the water depth varies, the wave period, T remains constant. Since the wave period is constant, it follows from (2.15) and (2.16) that as waves propagate from deep to shallow water, the phase speed, C and the wave length, L will both decrease.

The basic assumptions to be invoked in considering wave transformation can be summarized as:

1. The bottom slope varies slowly.
2. Energy transmission between adjacent orthogonals (i.e. line perpendicular to the wave crest) is constant.
3. The waves do not break.
4. The wave period, T and hence frequency, f or ω are constant.

2.3.2 Wave Shoaling

Initially, consider the two-dimensional problem of waves at normal incidence to straight parallel depth contours as shown in Figure 2.7. The energy of a wave per

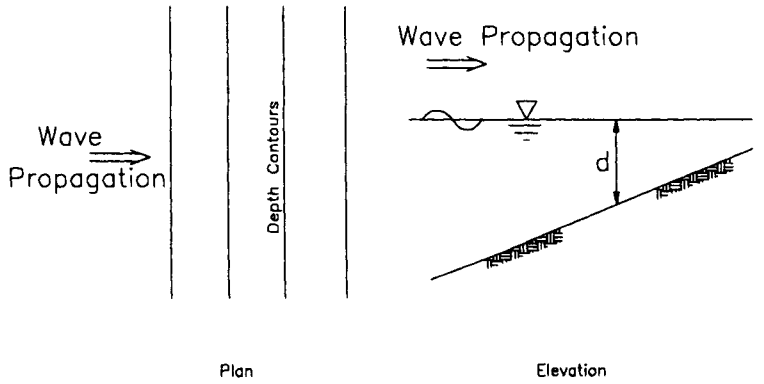

Figure 2.7: Definition sketch showing the two-dimensional shoaling of linear water waves.

unit crest length can be shown to be [Dean and Dalrymple (1991) and many others]

$$E = \frac{1}{8}\rho_w g H^2 L \tag{2.36}$$

The energy per unit area or specific energy is

$$\overline{E} = \frac{1}{8}\rho_w g H^2 \tag{2.37}$$

The energy flux, $\overline{P}$, is the rate at which the wave energy is advected. From Section (2.2.9), the energy is advected at the group velocity, C_g.

$$\overline{P} = \overline{E}C_g = \overline{E}nC \tag{2.38}$$

The energy flux, $\overline{P}$ is also called the wave power. Since the amount of energy entering a region must equal the amount leaving (conservation of energy) it follows that

$$\overline{E}_0 n_0 C_0 = \overline{E} n C \tag{2.39}$$

where the zero subscripts refer to deep water values. From (2.37) and (2.39) it follows that

$$\frac{H}{H_0} = K_s = \sqrt{\frac{n_0 C_0}{nC}} \tag{2.40}$$

The quantity K_s is called the *Shoaling Coefficient*. As shown in Figure 2.8, with decreasing water depth the shoaling coefficient decreases slightly below one before increasing rapidly. As stated in Section (2.3.1), the wave length also decreases with decreasing water depth. Hence, as the waves propagate into progressively shallower water, the wave slope, H/L will increase. As the steepness increases, the waves will reach a point where their form is unstable and they will begin to break.

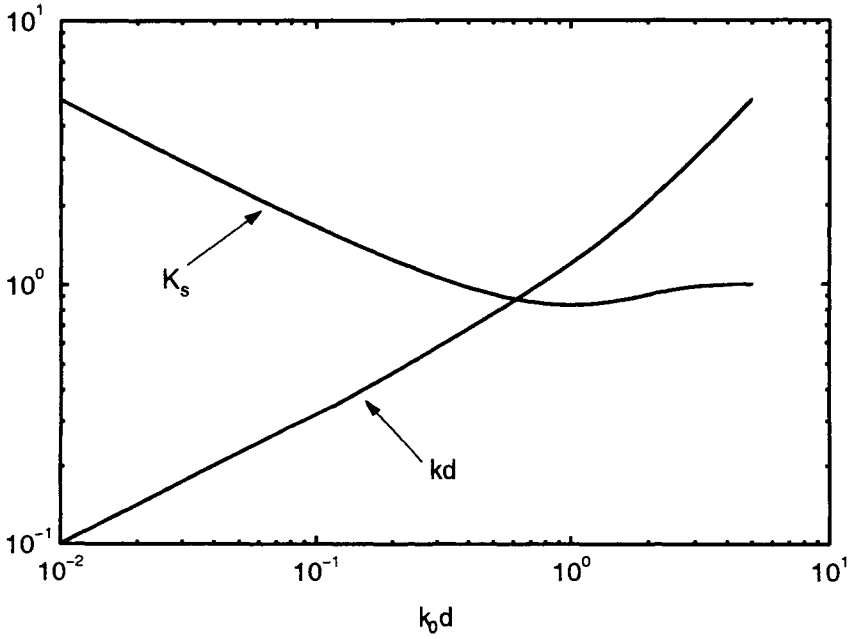

Figure 2.8: Variation in the shoaling coefficient, K_s and the non-dimensional depth parameter, kd as a function of $k_0 d$, where k_0 is the deep water wave number.

2.3.3 Wave Refraction

Equation (2.15) indicates that the phase speed, C varies as a function of the water depth, d. Therefore, for a wave which is approaching the depth contours of Figure 2.7 at an angle other than normal, the water depth will vary along the wave

crest. Therefore, the phase speed will also vary along the wave crest. As a result, the crest will tend to bend towards alignment with the depth contours. Wave orthogonals which are normal to the wave crest will not be straight lines but will bend as the crest bends. As a result, adjacent orthogonals may converge or diverge depending on the local bathymetry as shown in Figure 2.9.

A simple extension of (2.38) to this three-dimensional case yields

$$\overline{P} = \overline{E}nCb = \text{constant} \tag{2.41}$$

where b is the spacing between adjacent orthogonals (see Figure 2.9). Equation (2.41) assumes that there is no lateral transport of energy along the wave crests. It follows that the wave height variation is

$$\begin{aligned} \frac{H}{H_0} &= \sqrt{\frac{n_0 C_0}{nC}}\sqrt{\frac{b_0}{b}} \\ &= K_s K_r \end{aligned} \tag{2.42}$$

where K_r is termed the refraction coefficient. Whereas K_s can be evaluated from linear wave relationships in deep water and at the point of interest, K_r requires knowledge of the paths adjacent orthogonals have taken in propagating from deep water to the point of interest.

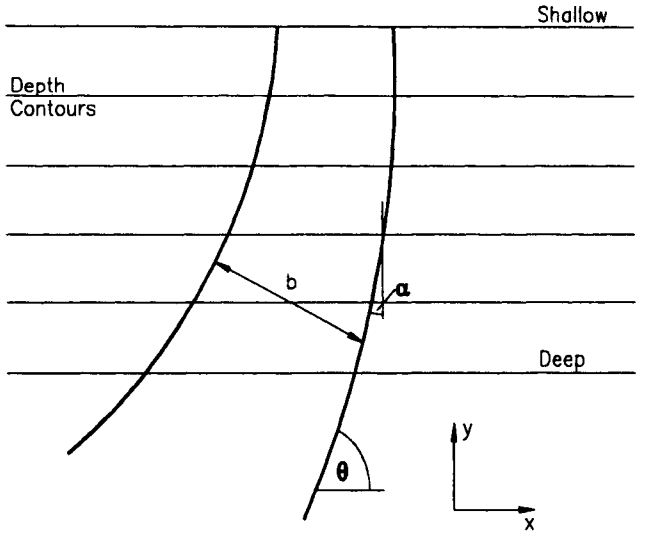

Figure 2.9: Definition sketch showing the refraction of waves over parallel depth contours. The wave orthogonals are shown by the bold lines.

Munk and Arthur (1952) have shown that the orthogonal or wave ray is defined

by

$$\begin{aligned} \frac{ds}{dt} &= C \\ \frac{dx}{dt} &= C\cos\theta \\ \frac{dy}{dt} &= C\sin\theta \end{aligned} \tag{2.43}$$

where x and y are the standard coordinate directions, θ is the local direction of wave propagation and s is the coordinate direction along the wave ray (see Figure 2.9). In general, (2.43) must be solved numerically by stepping along the wave ray. For the case of parallel bed contours, however, an analytical solution in the form of Snel's law results

$$\frac{\sin\alpha}{C} = \text{constant} \tag{2.44}$$

where α is the angle between the wave ray and a normal to the bed contour. Historically, (2.44) has been applied to cases other than parallel bed contours and allowed the graphical construction of refraction diagrams. This process was extremely time consuming and prone to inaccuracy. It has now been replaced by numerical solutions to (2.43).

Snel's law is commonly encountered in the field of geometric optics and the analogy between the refraction of light and that of water waves is compelling. For light, it is the change in the refractive index of the medium which is responsible for refraction. For water waves, the change in water depth has the same effect.

2.4 Limitations of Linear Wave Theory

The wave theory developed in Section (2.2) assumed that the wave height was so small that the dynamic and kinematic boundary conditions at the free surface [(2.5) and (2.7)] could be applied at the still water level, $z = 0$ rather than at the wave disturbed surface $z = \eta$. In nature, the wave steepness, H/L seldom exceeds 0.05 to 0.08 (Svendsen and Jonsson, 1976) and hence the small amplitude assumption is often valid. There are, however, some applications where the simplifying assumptions of Linear Wave Theory become significant. In such cases it is necessary to resort to the use of a non-linear or *finite amplitude wave theory*. Such theories require the free surface boundary conditions to be applied at the free surface, which is, initially unknown as the wave form is part of the solution. The problem is made tractable by the use of *perturbation methods*. Such an analysis assumes that the non-linearities represent only small corrections to linear wave theory.

Physically the difference between linear and finite amplitude theories is that finite amplitude theories consider the influence of the wave itself on its properties. Therefore, in contrast to linear theory, the phase speed, wave length, water surface profile and other properties are functions of the actual wave height.

There are a number of different finite amplitude wave theories which have been proposed, but the two most commonly adopted theories are: *Stokes' Wave Theory* (Stokes, 1847, 1880; Miche, 1944) and *Cnoidal Wave Theory* (Korteweg and De Vries, 1895; Keulegan and Patterson, 1940; Wiegel, 1960). Stokes' theory is applicable in deep water whereas Cnoidal theory applies in finite depth situations.

Linear wave theory predicts that the crest and trough heights of the wave are equal. That is, the wave is evenly distributed about the still water level. In contrast, finite amplitude theories predict waves with peaked crests and flat troughs. The crests are further above the still water level than the troughs are below this level. Hence, in applications such as determining the deck elevation of an offshore structure, the use of finite amplitude wave theory would be important. Linear wave theory predicts that water particles move in closed orbits. Hence, there is no net transport of fluid. In contrast, finite amplitude theory predicts a small net fluid transport in the direction of wave propagation.

Despite the sophistication of finite amplitude wave theory, it still predicts waves which are of essentially a single period. There is a clear wave period and length. In reality, this seldom occurs in the ocean. Successive waves typically vary in height, period and propagation direction. Therefore, even high order finite amplitude theory is limited in such cases.

2.5 Spectral Representation of Waves

2.5.1 Frequency or Omni-directional Spectrum

Even the most casual observer of ocean waves would have realized that the simplifying assumptions of a constant wave period and waves of constant form place significant limitations on linear or finite amplitude wave theories. Waves typically appear confused with successive heights, periods and wave lengths varying significantly. Indeed, in some cases the actual direction of propagation is also difficult to define with confidence. The water surface appears confused rather than conforming to an ordered sinusoidal form as predicted by (2.11). An example of this is shown by the typical recorded wave record shown in Figure 2.10.

In many areas of physics it is common to represent records such as that of Figure 2.10 by the use of a spectral or Fourier model. Under this approximation, the water surface elevation is approximated by the linear superposition of sinusoidal forms as defined by (2.11).

$$\eta(t) = \sum_{i=1}^{N} a_i \sin(\omega_i t + \phi_i) \tag{2.45}$$

where a_i, ω_i and ϕ_i are the amplitude, frequency and phase of the ith component in the summation. An example of the manner in which a complex water surface

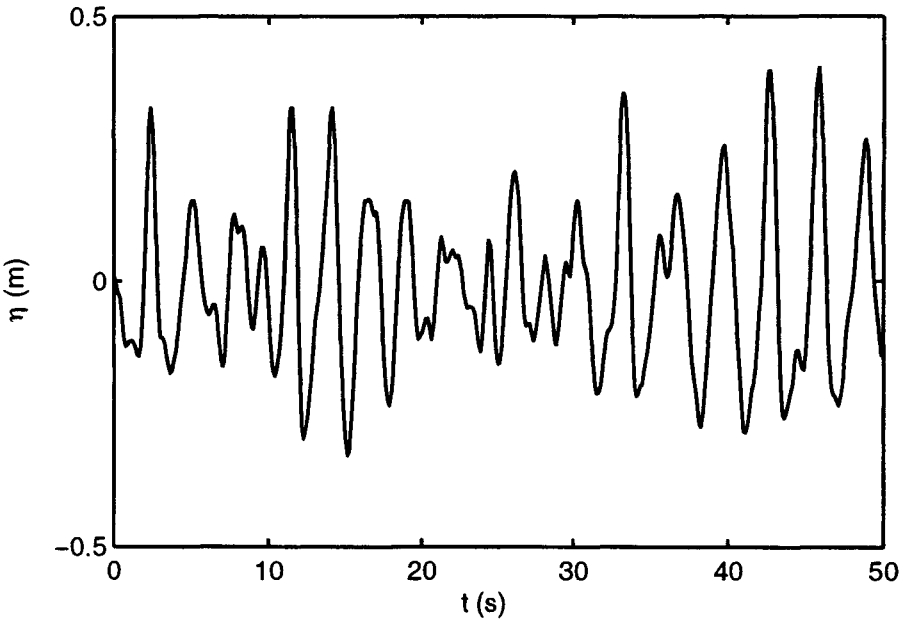

Figure 2.10: A typical wave record measured at Lake George, Australia in a water depth of approximately 2m. The wind speed was, U_{10}=16.3m/s. Note the variation in height and period of individual waves in the record.

record can be constructed from the summation of only 3 sinusoids is shown in Figure 2.11.

Each of the sinusoidal components in the summation (2.45) will satisfy all the properties of linear wave theory as developed in Sections (2.2.3) to (2.2.7).

From (2.37), the average energy of the wave profile can be represented as

$$\overline{E} = \frac{\rho_w g}{8} \sum_{i=1}^{N} H_i^2 \tag{2.46}$$

or

$$\frac{\overline{E}}{\rho_w g} = \frac{1}{2N} \sum_{i=1}^{N} a_i^2 = \sigma^2 \tag{2.47}$$

where σ^2 is the variance of the record.

Therefore, the amplitude components, a_i^2 are related to the energy of the record, the distribution of which as a function of frequency could be represented by plotting a_i^2 verses frequency as shown in Figure 2.12a. This amplitude spectrum is discrete, represented only at the frequencies ω_i of the summation (2.45). In the limit as $N \rightarrow \infty$ the amplitude spectrum can be transformed into the continuous spectrum,

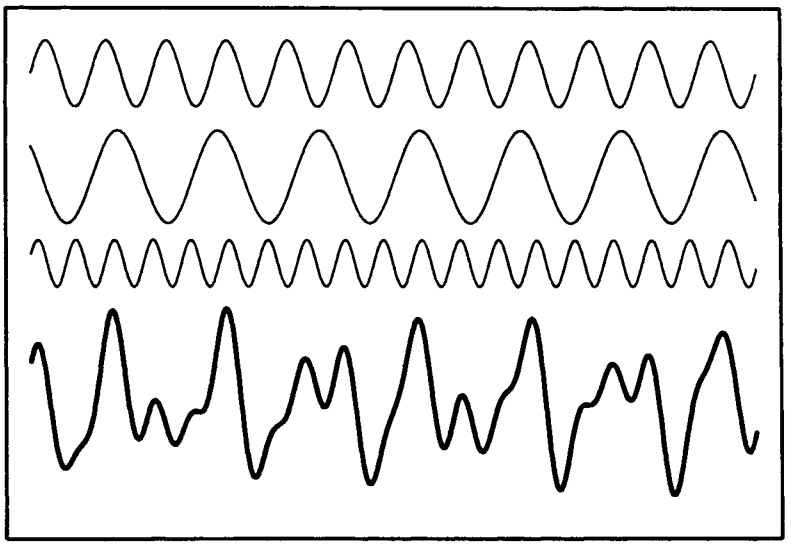

Figure 2.11: Construction of a complex water surface elevation record from the summation of three sinusoidal forms as represented by (2.45). The three sinusoidal records at the top (thin lines) sum to yield the record at the bottom (thick line).

$F(f)$, where

$$F(f)\Delta f = \frac{a_i^2}{2} \tag{2.48}$$

The spectrum, $F(f)$ is called the frequency or omni-directional [as no direction is associated with the spectrum - see Section (2.5.2)] or variance [as the area under the spectrum is the variance f the record] spectrum.

$$\sigma^2 = \int_0^\infty F(f)\mathrm{d}f \tag{2.49}$$

The use of the variance spectrum has the advantage that complex water surface elevation records can be considered, whilst retaining the compelling simplicity of linear wave theory. Examination of (2.45), however, reveals that the phase information represented by the ϕ_i terms have been discarded in forming the spectrum. As is evident in Figure 2.11, the choice of the values of ϕ_i will influence the resulting water surface elevation. The selection of the values of ϕ_i will, however, have no influence on the spectrum. Hence, the spectrum defines the distribution of energy with frequency but does not describe the actual water surface elevation unless additional assumptions about the associated "phase spectrum" are adopted.

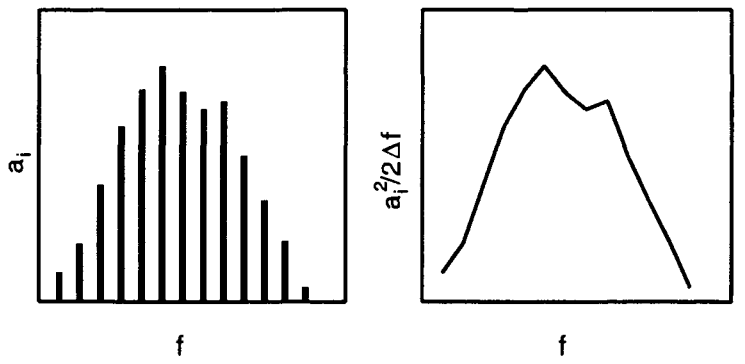

Figure 2.12: Illustrations of (a) the discrete amplitude spectrum (left) and (b) the continuous frequency or variance spectrum (right).

2.5.2 Directional Spectrum

A further extension of the Fourier model represented by (2.45) is to also include the possibility of wave components propagating in different directions

$$\eta(x,y,t) = \sum_{i=1}^{N} a_i \sin\left[k_i\left(x\cos\theta_i + y\sin\theta_i\right) - \omega_i t + \phi_i\right] \tag{2.50}$$

where θ_i is the angle between the x axis and the direction of propagation of the ith component in the summation. From this representation, a frequency-direction or directional spectrum, $F(f,\theta)$ can be defined in a similar manner to $F(f)$.

$$\sigma^2 = \int_0^{2\pi}\int_0^{\infty} F(f,\theta)\mathrm{d}f\mathrm{d}\theta \tag{2.51}$$

The directional frequency spectrum defines the distribution of energy with frequency and direction. From (2.50) it follows that this distribution could have been alternatively written in terms of wave number, thus forming a wave number spectrum $Q(k_x,k_y)$, where k_x and k_y are the wave number components in the x and y directions respectively. The wave number spectrum can be related to the directional frequency spectrum since

$$\sigma^2 = \int\int Q(k_x,k_y)\mathrm{d}k_x\mathrm{d}k_y = \int\int F(f,\theta)\mathrm{d}f\mathrm{d}\theta \tag{2.52}$$

Noting that $\mathrm{d}k_x\mathrm{d}k_y = |\boldsymbol{k}|\mathrm{d}k\mathrm{d}\theta$, this yields

$$F(f,\theta) = Q(k_x,k_y)|\boldsymbol{k}|\frac{\mathrm{d}k}{\mathrm{d}f} \tag{2.53}$$

where $\mathrm{d}k/\mathrm{d}f$ can be determined from the dispersion relationship (2.13).